

# Electronic spectroscopy, lifetimes, and barrier to linearity in the $\tilde{A}^1B_1 \leftarrow \tilde{X}^1A_1$ system of dibromocarbene

Chong Tao, Calvin Mukarakate, Danielle Brusse, Yulia Mishchenko, Scott A. Reid \*

Department of Chemistry, Marquette University, Milwaukee, WI 53201-1881, USA

Received 5 December 2006; in revised form 11 December 2006

Available online 22 December 2006

## Abstract

Using an improved discharge recipe for the production of dibromocarbene ( $\text{CBr}_2$ ), we recently reassigned the electronic origin of the  $\tilde{A}^1B_1 \leftarrow \tilde{X}^1A_1$  system, based on an extensive data set of isotope shifts for the pure bending transitions [C. Tao, C. Mukarakate, D. Brusse, Y. Mishchenko, S. A. Reid, *J. Mol. Spectrosc.* 240 (2006) 139–140]. In this study, we report the complete analysis of the fluorescence excitation spectrum of the  $\tilde{A}^1B_1 \leftarrow \tilde{X}^1A_1$  system in the 525–650 nm region, obtained at a rotational temperature of  $\sim 10$  K. A total of 32 cold bands involving the pure bending levels  $2_0^n$  with  $n = 2$ –19 and combination bands  $1_0^1 2_0^n$  ( $n = 1$ –16) in the  $\tilde{A}^1B_1 \leftarrow \tilde{X}^1A_1$  system were observed; a number of these are reported here for the first time. Rotational analysis typically yielded  $A$  rotational constants and band origins for all three bromine isotopomers ( $\text{C}^{79}\text{Br}_2$ ,  $\text{C}^{79}\text{Br}^{81}\text{Br}$ ,  $\text{C}^{81}\text{Br}_2$ ), and Dunham expansion fits yielded an extensive set of vibrational parameters for each. The isotope shifts are in good agreement with the product rule, and, when plotted vs. bending quantum number, the measured  $A$  constants follow a linear trend except for the highest bending levels, where an abrupt increase is observed, indicative of the approach to linearity. This is mirrored in the vibrational intervals, which also change abruptly in this region, and the estimated barrier height of  $\sim 18800$   $\text{cm}^{-1}$  above the vibrationless level of the  $\tilde{X}^1A_1$  state is in excellent agreement with the *ab initio* prediction of Sendt and Bacskay [K. Sendt, G.B. Bacskay, *J. Chem. Phys.* 112 (2000) 2227–2238]. We also report fluorescence lifetimes as a function of vibrational level and  $K'_a$ ; the lifetimes decrease rapidly with energy, but display no dependence on  $K'_a$  over the measured range. The implications of these results for understanding the excited state structure of this prototypical carbene are emphasized.

© 2006 Elsevier Inc. All rights reserved.

**Keywords:** Carbenes; Electronic spectroscopy; Renner–Teller effect; Fluorescence lifetimes; Dibromocarbene; Barrier to linearity; Fluorescence spectroscopy

## 1. Introduction

Carbenes are among the most important of reactive intermediates [1], and there is much current interest in their spectroscopy, photochemistry, and photophysics. With a divalent carbon, carbenes have low-lying singlet and triplet configurations of similar energy but very different reactivity, and the magnitude of the singlet–triplet gap ( $\Delta E_{\text{ST}}$ ) is an important quantity needed to predict their reactivity in environments where both states can be populated. Small halocarbenes  $\text{CXY}$  ( $\text{X} = \text{H}, \text{F}, \text{Cl}, \text{Br}$ ;  $\text{Y} = \text{F}, \text{Cl}, \text{Br}$ ) have served as excellent benchmarks for comparing experimen-

tal and theoretically derived  $\Delta E_{\text{ST}}$ s, and recent progress has been made in determining  $\Delta E_{\text{ST}}$  for a number of these systems [2–17]. As the smallest carbenes with singlet ground states, the halocarbenes are also of interest in unraveling the complicated interplay of anharmonic, Renner–Teller (RT), and spin–orbit couplings typically observed in the spectroscopy of these molecules [18–20].

While reactions of dibromocarbene ( $\text{CBr}_2$ ) have been known for decades [21], considerably less is known regarding the electronic spectroscopy of  $\text{CBr}_2$  than that of the other symmetric dihalocarbenes  $\text{CF}_2$  and  $\text{CCl}_2$ . Previously, electronic spectra have been obtained in both gas-phase and matrix environments [22–28], yet important questions still remain. Following the development of an improved discharge recipe for production of this carbene largely free

\* Corresponding author. Fax: +1 414 288 7066.

E-mail address: scott.reid@mu.edu (S.A. Reid).

from interference of  $\text{CHBr}$  or  $\text{Br}_2$ , we have recently recorded and rotationally analyzed the complete visible fluorescence excitation spectrum of  $\text{CBr}_2$ , which led to a revision in the assignment of the electronic origin of this system [29]. We have also measured extensive single vibronic level emission spectra of this system, in order to probe for spin–orbit interactions and the singlet–triplet gap [30]. In this report, we present the complete results of our analysis of the  $\tilde{A}^1B_1 \leftarrow \tilde{X}^1A_1$  system, focusing on the excited state structure and barrier to linearity.

## 2. Experimental section

The apparatus, pulsed discharge nozzle, and data acquisition procedures have been described in detail in earlier studies [15–17], and the specific conditions for optimizing the production of  $\text{CBr}_2$  were described in a recent paper [29]. Briefly, we produced  $\text{CBr}_2$  through a mixture of  $\text{CBr}_4$ ,  $\text{CHBr}_3$ , and Ar, generated by passing pure Ar at a pressure of  $\sim 2$  bar through a stainless steel bubbler containing a solution of  $\text{CBr}_4$  (Aldrich, 99%) in  $\text{CHBr}_3$  (Aldrich, 99%) at room temperature. The discharge was initiated by a +1 kV pulse of  $\sim 100$   $\mu\text{s}$  duration, through a current limiting 10 k $\Omega$  ballast resistor. The timing of laser, nozzle, and discharge firing was controlled by a digital delay generator (Stanford Research Systems DG535), which also generated a variable width gate pulse for the high voltage pulser (Directed Energy GRX-1.5K-E). The laser system consisted of an etalon narrowed dye laser (Lambda-Physik Scanmate 2E) pumped by the second or third harmonic of a Nd:YAG laser (Continuum NY-61). The laser beam was not focused, and typical pulse energies were  $\sim 1$ –2 mJ in a  $\sim 3$  mm diameter beam.

These measurements utilized a mutually orthogonal geometry of laser, molecular beam, and detector, where the laser beam crossed the molecular beam at a distance of  $\sim 10$  mm downstream. Fluorescence was collected and collimated by a 2 in. diameter  $f/2.4$  plano-convex lens (UV-grade fused silica), and focused onto the photomultiplier tube (PMT) detector using a 2 in. diameter  $f/3.0$  plano-convex lens (also UV-grade fused silica). The fluorescence was filtered via an appropriate long-pass cutoff filter (Corion or Edmund Scientific) prior to striking a photomultiplier tube detector (Oriel) held at typically  $-700$  V. A portion of the laser beam was directed into a Fe:Ne hollow cathode lamp for wavelength calibration via the optogalvanic effect. The PMT and optogalvanic signals were simultaneously integrated using a two channel gated integrator system (Stanford Research Systems 250), and the signal was passed to a personal computer through a 12 bit analog to digital converter. Typically, the signals from twenty to thirty laser shots were averaged at each step in wavelength (0.002 nm). Spectra were calibrated to vacuum wavenumbers using line positions from the NIST atomic spectral database [31]. The spectra were simulated based on the positions of the sharp  ${}^rR_K$  bandheads, using the AsyrotWin program package of Judge and Clouthier [32]. In these simulations the term energy

and  $A'$  constant were varied to match the experimental spectra, with the  $B'$  and  $C'$  constants fixed at the *ab initio* values. [33] We assumed identical rotational constants for each isotopomer in a given band.

## 3. Results and discussion

We obtained and rotationally analyzed fluorescence excitation spectra of 32 cold bands involving the pure bending levels  $2_0^n$  with  $n = 2$ –19 and combination bands  $1_0^1 2_0^n$  with  $n = 1$ –16 in the  $\tilde{A}^1B_1 \leftarrow \tilde{X}^1A_1$  system. Fig. 1 presents a survey scan of the entire spectrum; this extends across the range of several dyes, and was not normalized to laser power. In Fig. 2, we present an expanded view of the  $2_0^9$  band which compares experimental and simulated spectra; the individual simulations for each isotopomer ( $\text{C}^{79}\text{Br}_2$ ,  $\text{C}^{79}\text{Br}^{81}\text{Br}$ ,  $\text{C}^{81}\text{Br}_2$ ) are also shown. The isotopomer spectra are scaled in a 1:2:1 ratio, and the total (added) spectrum is scaled to match the experimental intensity. The derived spectral parameters for bands not previously reported [29] are listed in Table 1 along with estimated uncertainties. Where they overlap, these values are in good agreement with those reported by Xu and Harmony (XH) [26]; the deviations are less than  $1 \text{ cm}^{-1}$  in most cases. In presenting our results, we will focus on four aspects: (1) the excited state term energies, (2) the variation in  $A'$  with energy, (3) the excited state isotope shifts, and (4) the fluorescence lifetimes.

The term energies were fit using a nonlinear least squares routine to an anharmonic potential function (Dunham expansion) of the specific form [34]:

$$G^0(v_1, v_2) = T_{00} + v_1 v_1^0 + v_2 \omega_2^0 + v_1 v_2 x_{12}^0 + (v_2)^2 x_{22}^0 \quad (1)$$

where:  $T_{00}$  is the electronic origin,  $v_1^0$  is the anharmonic symmetric stretching frequency,  $\omega_2^0$  is the harmonic frequency of  $v_2$  (bend),  $x_{22}^0$  is a diagonal anharmonicity constant, and  $x_{12}^0$  is an off-diagonal or cross-anharmonicity

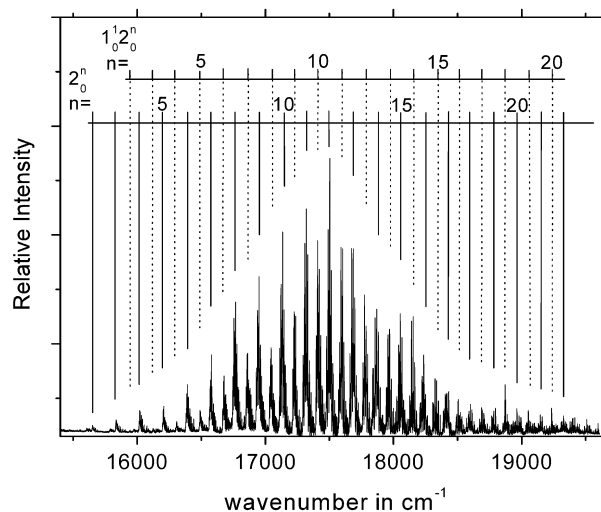


Fig. 1. Fluorescence excitation survey spectrum of the  $\tilde{A}^1B_1 \leftarrow \tilde{X}^1A_1$  system of  $\text{CBr}_2$ . Band assignments are noted.

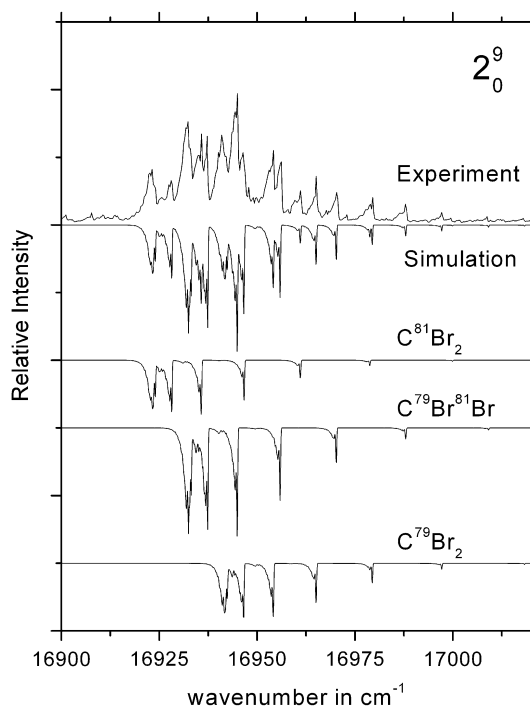


Fig. 2. Experimental (top) and simulated fluorescence excitation spectrum of the  $2_0^9$  band. The individual simulations for the three isotopomers are shown; these were added in a  $\sim 1:2:1$  ratio and the summed spectrum scaled to match the experiment. The rotational temperature is 10 K.

constant. As only transitions involving one quantum of symmetric stretch were observed, the harmonic frequency and diagonal anharmonicity for this mode could not be determined. The fit deviations are given in Table 1; using the  $C^{79}Br^{81}Br$  data set as an example, the fit to 30 levels returned a standard deviation of  $0.44 \text{ cm}^{-1}$ . The fit deviations for the two other isotopomers were slightly larger ( $\sim 0.5 \text{ cm}^{-1}$ ). In Table 2, we compare the derived parameters for all three isotopomers with the values of XH [26] and theoretical estimates [33,35]. Note that the electronic origins of the three isotopomers are the same to well within the experimental uncertainty, and the experimental frequencies lie between *ab initio* estimates at the CASSCF/cc-pVTZ and CASPT2/cc-pVTZ levels [33]. The diagonal anharmonicity  $x_{22}^0$  is very small, indicating that the bending mode in the excited state is nearly harmonic; a similar finding was reported for  $CCl_2$  [36]. Overall, our vibrational parameters are similar to those of XH [26], but more precise due to the larger data set employed.

The vibrational frequencies given in Table 2 follow the isotope shifts expected from the product rule. Considering the symmetrical isotopomers ( $C^{79}Br_2$ ,  $C^{81}Br_2$ ), the product rule predicts [34]:

$$\left( \frac{\omega_1^{C^{81}Br_2} \omega_2^{C^{81}Br_2}}{\omega_1^{C^{79}Br_2} \omega_2^{C^{79}Br_2}} \right)^2 = \frac{(2m_{81Br} + m_{12C}) (m_{79Br})^2}{(2m_{79Br} + m_{12C}) (m_{81Br})^2}. \quad (2)$$

Table 1  
Band origins,  $A$  rotational constants, and Dunham expansion fit deviations for the  $CBr_2$  bands measured in this work

Band	$A$ ( $\text{cm}^{-1}$ ) <sup>a</sup>	$C^{81}Br_2$		$C^{79}Br^{81}Br$		$C^{79}Br_2$	
		$T^b$	o. – c. <sup>c</sup>	$T$	o. – c.	$T$	o. – c.
$1_0^1 2_0^1$	2.81	...	...	15935.2	–0.2	...	...
$1_0^1 2_0^2$	2.86	...	...	16119.4	0.4	...	...
$1_0^1 2_0^3$	2.89	16299.1	0.2	16302.9	0.4	16306.5	0.5
$1_0^1 2_0^4$	2.94	16481.4	0.1	16485.8	–0.1	16490.4	0.0
$1_0^1 2_0^5$	3.01	16663.6	–0.1	16669.2	–0.1	16674.7	–0.2
$1_0^1 2_0^6$	3.05	16845.7	–0.3	16852.4	–0.3	16858.9	–0.3
$1_0^1 2_0^7$	3.08	17028.0	–0.3	17035.8	–0.2	17043.3	–0.2
$1_0^1 2_0^8$	3.13	17210.0	–0.5	17218.5	–0.7	17227.2	–0.6
$1_0^1 2_0^9$	3.15	17392.9	0.1	17402.5	0.1	17412.1	0.1
$1_0^1 2_0^{10}$	3.20	17574.9	0.0	17585.3	–0.3	17596.0	–0.2
$1_0^1 2_0^{11}$	3.24	17757.6	0.6	17769.2	0.5	17780.9	0.6
$1_0^1 2_0^{12}$	3.28	17939.1	0.0	17951.8	0.1	17964.6	0.3
$1_0^1 2_0^{13}$	3.32	18121.6	1.0	18135.1	0.4	18148.7	0.4
$1_0^1 2_0^{14}$	3.36	18303.4	0.5	18318.1	0.4	18332.5	0.2
$1_0^1 2_0^{15}$	3.40	18484.7	–0.4	18500.5	0.0	18516.0	–0.2
$2_0^{18}$	3.32	...	...	18579.9	...	...	...
$1_0^1 2_0^{16}$	3.45	18666.3	–0.7	18683.0	–0.5	18699.5	–0.5
$2_0^{19}$	3.60	18742.3	...	18761.3	...	18780.3	...

Parameters for the  $2_0^n$  bands with  $n = 2$ –17 were reported in Ref. [29].

<sup>a</sup> Estimated uncertainty of  $\pm 0.02 \text{ cm}^{-1}$ .

<sup>b</sup> Term energy; estimated uncertainty of  $\pm 0.2 \text{ cm}^{-1}$ .

<sup>c</sup> Observed – calculated.

Table 2  
Parameters for  $\text{CBr}_2$  ( $\tilde{A}^1B_1$ )

	$T_{00}$	$v_1^0$	$\omega_2^0$	$x_{12}^0$	$x_{22}^0$	Reference
<i>Experiment</i>						
$\text{C}^{81}\text{Br}_2$	15 278.78(48)	472.57(46)	183.11(11)	−0.539(44)	−0.021(6)	This work
	15 092.7(16)	473.8(12)	183.6(4)	−0.62(13)	−0.038(20)	[26]
$\text{C}^{79}\text{Br}^{81}\text{Br}$	15 278.86(38)	472.99(35)	184.13(8)	−0.519(35)	−0.024(4)	This work
	15 091.5(5)	475.0(5)	184.9(1)	−0.71(7)	−0.058(9)	[26]
$\text{C}^{79}\text{Br}_2$	15 278.67(46)	473.58(44)	185.19(11)	−0.537(42)	−0.026(5)	This work
	15 092.5(17)	474.8(12)	185.5(4)	−0.62(13)	−0.040(21)	[26]
<i>Theory</i>						
MRCI	15 237					[33]
CASSCF	16 486	444.6	177.9			[33]
CASPT2	14 191	484.0	194.6			[33]
CASPT2	15 192					[35]

The values derived in this work are compared with previous experimental values and theoretical estimates.

The right hand side of Eq. (2) is solely determined by the atomic masses, and has a value of 0.9736. Using our derived Dunham fit parameters (Table 2), the left-hand side has the value 0.9735(60), in excellent agreement.

The term energies for the  $2_0^{18}$  and  $2_0^{19}$  bands were excluded from our Dunham fits, because these alone exhibit large deviations (5.5 and 7.4  $\text{cm}^{-1}$ , respectively, for the  $\text{C}^{79}\text{Br}^{81}\text{Br}$  isotopomer) from the values predicted based upon the parameters in Table 2. Note that these are more than an order of magnitude larger than the overall fit standard deviation (0.44  $\text{cm}^{-1}$ ). As originally described by Dixon [37], and demonstrated experimentally for other triatomic carbenes with large barriers to linearity [38–41], deviations from the anharmonic model [Eq. (1)] reflect changes in the vibrational spacings upon the approach to

linearity. This finding is consistent with an increase in the  $A'$  constant for the pure bending levels which occurs in the same region; Fig. 3 displays a plot of the measured  $A'$  constants vs. quanta of bending excitation which shows the striking deviation from linear behavior observed for  $2_0^{18}$  and  $2_0^{19}$ . Our data suggests that the barrier to linearity occurs in the vicinity of  $2_0^{19}$ , or  $\sim 18800 \text{ cm}^{-1}$ , consistent with the *ab initio* estimate (CASPT2[g<sub>1</sub>]/cc-pVTZ level) of  $\sim 19065 \text{ cm}^{-1}$  [33].

The majority of measured  $A'$  constants (Fig. 3) show a linear dependence when plotted vs. bending quanta, as noted previously by XH. For these data, a linear regression fit to the expression [42]:

$$A'(v'_1, v'_2) = A'_{\text{eq}} - (v'_1 + 1/2)\alpha'_1 - (v'_2 + 1/2)\alpha'_2 \quad (3)$$

returns the fit parameters:  $A'_{\text{eq}} = 2.543(16) \text{ cm}^{-1}$ ,  $\alpha'_1 = -0.176(10) \text{ cm}^{-1}$ , and  $\alpha'_2 = -0.037(1) \text{ cm}^{-1}$ . The  $A'_{\text{eq}}$  value lies between *ab initio* estimates of 2.458  $\text{cm}^{-1}$  (CASSCF/cc-pVTZ level) and 2.949  $\text{cm}^{-1}$  (CASPT2/cc-pVTZ level) [33]. As  $\bar{B}'$  is rather insensitive to bond angle and  $A'$  to bond length, using the *ab initio* (CASPT2/cc-pVTZ) value of  $R_{\text{C-Br}} = 1.800 \text{ \AA}$  we estimate a bond angle  $\theta'_0 = 131.3^\circ$  for the vibrationless level of the  $\tilde{A}^1B_1$  state.

We have previously reported excited state isotope shifts for the pure bending progression ( $2_0^n$ ), which led to our reassignment of the electronic origin of this system [29]. Within the harmonic approximation, the isotope shifts for a pair of isotopomers follow a linear relationship expressed by [26]:

$$\Delta T_{0v'_2} = \Delta T_{00} + (\Delta\omega_2^0)v'_2, \quad (4)$$

where:  $\Delta T_{00}$  is the difference in isotope shift of the vibrationless levels in the two electronic states, and  $\Delta\omega_2^0$  is the difference in harmonic bending frequency for the two isotopomers. Fig. 4 shows a comparison of the  $\text{C}^{79}\text{Br}_2$ – $\text{C}^{81}\text{Br}_2$  isotope shifts for the  $2_0^n$  (upper panel) and  $1_0^1 2_0^n$  progressions. The expected linear dependence is observed, and the derived parameters [ $2_0^n$ :  $\Delta T_{00} = -0.02(12) \text{ cm}^{-1}$ ,  $\Delta\omega_2^0 = 2.027(11) \text{ cm}^{-1}$ ;  $1_0^1 2_0^n$ :  $\Delta T_{00} =$

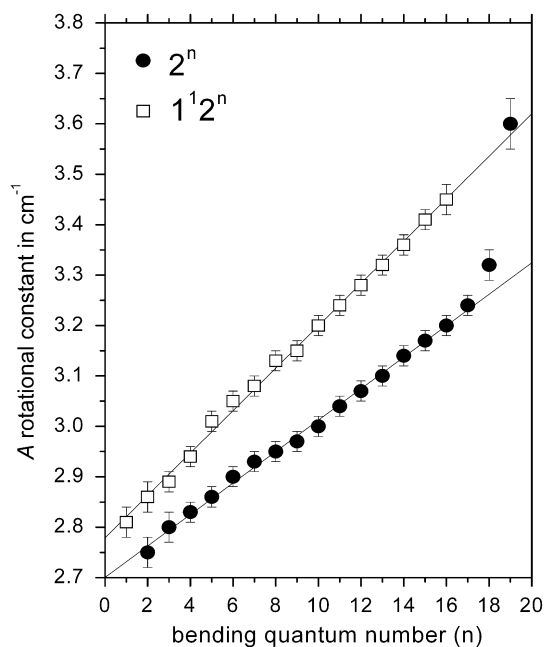


Fig. 3. Measured  $A$  rotational constants for bands in the  $2^n$  and  $1^1 2^n$  progressions. In each case a linear dependence is observed, with the exception of the highest members ( $n = 18, 19$ ) of the  $2^n$  progression.

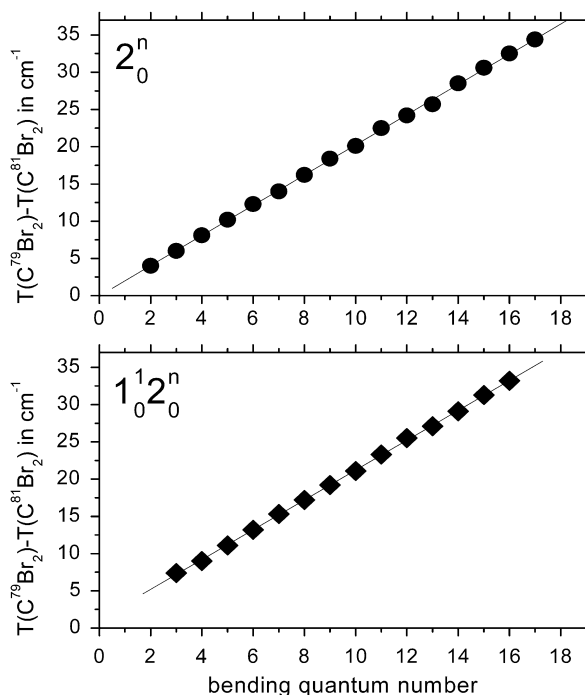


Fig. 4. Measured ( $C^{79}Br_2 - C^{81}Br_2$ ) isotope shifts for the  $2^n$  and  $1_0^{2n}$  progressions. In each case a linear dependence is observed.

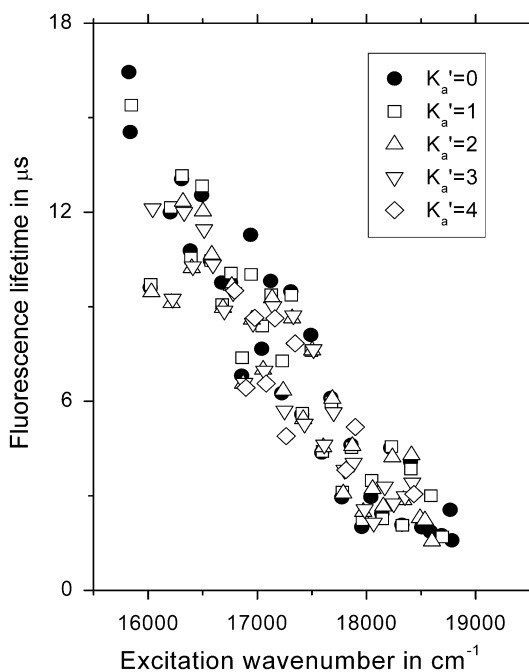


Fig. 5. Measured fluorescence lifetimes as a function of energy and  $K'_a$ . The lifetimes steadily decrease with increasing energy, but no dependence on  $K'_a$  is seen over this range.

$1.19(10) \text{ cm}^{-1} \Delta \omega_2^{0'} = 2.003(9) \text{ cm}^{-1}$ ] are consistent with the Dunham parameters in Table 2.

Fig. 5 shows a compilation of the fluorescence lifetimes measured in this work, which are sorted as a function of energy and  $K'_a$ . The lifetimes decrease significantly with energy, and the longest lifetime measured is  $\tau = 16.4(3) \mu\text{s}$

for  $2_0^3$ ,  $K'_a = 0$ . No significant dependence on  $K'_a$  is observed over this range. Comparing with previous data, Bondebey and English reported a lifetime of  $14.5 \mu\text{s}$  in an Ar matrix, roughly consistent with our result [24]. The only previous gas-phase measurement of which we are aware was that of Lee et al., who reported a lifetime of  $3.4(4) \mu\text{s}$  in the region between  $2_0^{14}$  and  $2_0^{16}$  (i.e.,  $\sim 17800$  to  $18200 \text{ cm}^{-1}$ ) [27]. This is also roughly consistent with our results. For other systems with a high barrier to linearity, namely CHF and CDF [39–41], we have observed lifetime lengthening for levels with  $K'_a > 0$  due to the Renner–Teller effect as the RT intersection is approached. For  $CBr_2$ , analysis of the barrier region is hampered by the small FC factors and interference from  $Br_2$  fluorescence, and lifetime lengthening cannot be clearly seen. However, other manifestations of the approach to the RT intersection (increase in A constant, change in vibrational intervals) are consistent with the trends observed for the other carbenes.

#### 4. Conclusions

Using an improved discharge recipe for the production of dibromocarbene ( $CBr_2$ ), we report the complete analysis of the fluorescence excitation spectrum of the  $\tilde{A}^1B_1 \leftarrow \tilde{X}^1A_1$  system in the 525–650 nm region, obtained at a rotational temperature of  $\sim 10 \text{ K}$ . A total of 32 cold bands involving the pure bending levels  $2_0^n$  with  $n = 2$ –19 and combination bands  $1_0^1 2_0^n$  ( $n = 1$ –16) in the  $\tilde{A}^1B_1 \leftarrow \tilde{X}^1A_1$  system were observed; a number of these are reported here for the first time. Rotational analysis typically yielded  $A$  rotational constants and band origins for all three bromine isotopomers ( $C^{79}Br_2$ ,  $C^{79}Br^{81}Br$ ,  $C^{81}Br_2$ ), and Dunham expansion fits yielded an extensive set of vibrational parameters for each. The isotope shifts are in good agreement with the product rule, and, when plotted vs. bending quantum number, the measured  $A$  constants follow a linear trend except for the highest bending levels, where an abrupt increase is observed, indicative of the approach to linearity. This effect is mirrored in the vibrational spacings, which also change abruptly in this region. The estimated barrier height is in excellent agreement with *ab initio* predictions [33]. We have also reported fluorescence lifetimes as a function of vibrational level and  $K'_a$ ; the lifetimes decrease rapidly with energy, but display no dependence on  $K'_a$  over the measured range.

#### Acknowledgment

The National Science Foundation (Grant CHE-0353596) is gratefully acknowledged for their support of this research.

#### References

- [1] See, e.g., R.A. Moss, M.S. Platz, M. Jones Jr. (Eds.), *Reactive Intermediate Chemistry*, Wiley-Interscience, Hoboken, NJ, 2004, Chapters 7–9.
- [2] K.K. Murray, D.G. Leopold, T.M. Miller, W.C. Lineberger, *J. Chem. Phys.* 89 (1988) 5442–5453.

- [3] M.K. Gilles, K.M. Ervin, J. Ho, W.C. Lineberger, *J. Phys. Chem.* 96 (1992) 1130–1141.
- [4] R.L. Schwartz, G.E. Davico, T.M. Ramond, W.C. Lineberger, *J. Phys. Chem. A* 103 (1999) 8213–8221.
- [5] C.-W. Chen, T.-C. Tsai, B.-C. Chang, *Chem. Phys. Lett.* 347 (2001) 73–78.
- [6] C.-W. Chen, T.-C. Tsai, B.-C. Chang, *J. Mol. Spectrosc.* 209 (2001) 254–258.
- [7] T.-C. Tsai, C.-W. Chen, B.-C. Chang, *J. Chem. Phys.* 115 (2001) 766–770.
- [8] H.-G. Yu, T. Lezana-Gonzalez, A.J. Marr, J.T. Muckerman, T.J. Sears, *J. Chem. Phys.* 115 (2001) 5433–5444.
- [9] C.-L. Lee, M.-L. Liu, B.-C. Chang, *J. Chem. Phys.* 117 (2002) 3263–3268.
- [10] C.-L. Lee, M.-L. Liu, B.-C. Chang, *Phys. Chem. Chem. Phys.* 5 (2003) 3859–3863.
- [11] M.-L. Liu, C.-L. Lee, A. Bezant, G. Tarczay, R.J. Clark, T.A. Miller, B.-C. Chang, *Phys. Chem. Chem. Phys.* 5 (2003) 1352–1358.
- [12] C.-S. Lin, Y.-E. Chen, B.-C. Chang, *J. Chem. Phys.* 121 (2004) 4164–4170.
- [13] W.-Z. Chang, H.-J. Hsu, B.-C. Chang, *Chem. Phys. Lett.* 413 (2005) 25–30.
- [14] G. Tarczay, T.A. Miller, G. Czako, A.G. Császár, *Phys. Chem. Chem. Phys.* 7 (2005) 2881–2893.
- [15] M. Deselnicu, C. Mukarakate, C. Tao, S.A. Reid, *J. Chem. Phys.* 124 (2006) 134302/1.
- [16] C. Tao, C. Mukarakate, S.A. Reid, *J. Chem. Phys.* 124 (2006) 224314/1–224314/11.
- [17] C. Tao, M. Deselnicu, C. Mukarakate, S.A. Reid, *J. Chem. Phys.* 125 (2006) 094305/1–094305/9.
- [18] A. Lin, K. Kobayashi, H.-G. Yu, G.E. Hall, J.T. Muckerman, T.J. Sears, A.J. Merer, *J. Mol. Spectrosc.* 214 (2002) 216–224.
- [19] B.-C. Chang, T.J. Sears, *J. Chem. Phys.* 105 (1996) 2135–2140.
- [20] I. Ionescu, H. Fan, E. Ionescu, S.A. Reid, *J. Chem. Phys.* 121 (2004) 8874–8879.
- [21] See, e.g. W.V. E. Doering, P. LaFlamme, *J. Am. Chem. Soc.* 78 (1956) 5447–5448.
- [22] L. Andrews, *J. Chem. Phys.* 48 (1968) 979–982.
- [23] L. Andrews, T.G. Carver, *J. Chem. Phys.* 49 (1968) 896–902.
- [24] V.E. Bondybey, J.H. English, *J. Mol. Spectrosc.* 79 (1980) 416–423.
- [25] S.K. Zhou, M.S. Zhan, J.L. Shi, C.X. Wang, *Chem. Phys. Lett.* 166 (1990) 547–550.
- [26] S. Xu, M.D. Harmony, *J. Phys. Chem.* 97 (1993) 7465–7470.
- [27] C.-L. Lee, M.-L. Liu, B.-C. Chang, *Phys. Chem. Chem. Phys.* 5 (2003) 3859–3863.
- [28] H.-J. Hsu, W.-Z. Chang, B.-C. Chang, *Phys. Chem. Chem. Phys.* 7 (2005) 2468–2473.
- [29] C. Tao, C. Mukarakate, D. Brusse, Y. Mishchenko, S.A. Reid, *J. Mol. Spectrosc.* 240 (2006) 139–140.
- [30] C. Tao, C. Mukarakate, S.A. Reid, *J. Mol. Spectrosc.* 241 (2007) 136–142.
- [31] NIST Atomic Spectra Database, V. 3.0 (<http://physics.nist.gov/PhysRefData/ASD>).
- [32] R.H. Judge, D.J. Clouthier, *Comput. Phys. Commun.* 135 (2001) 293–311.
- [33] K. Sendt, G.B. Bacskay, *J. Chem. Phys.* 112 (2000) 2227–2238.
- [34] G. Herzberg, *Molecular Spectra and Molecular Structure III. Electronic Spectra of Polyatomic Molecules*, Van Nostrand, New York, 1966.
- [35] S.A. Drake, J.M. Standard, R.W. Quandt, *J. Phys. Chem. A* 106 (2002) 1357–1364.
- [36] D.J. Clouthier, J. Karolczak, *J. Chem. Phys.* 94 (1991) 1–10.
- [37] R.N. Dixon, *Trans. Faraday Soc.* 60 (1964) 1363–1368.
- [38] T.W. Schmidt, G.B. Bacskay, S.H. Kable, *J. Chem. Phys.* 110 (1999) 11277–11285.
- [39] H. Fan, I. Ionescu, C. Annesley, S.A. Reid, *Chem. Phys. Lett.* 378 (2003) 548–552.
- [40] H. Fan, I. Ionescu, C. Annesley, J. Cummins, M. Bowers, J. Xin, S.A. Reid, *J. Phys. Chem. A* 108 (2004) 3732–3738.
- [41] C. Tao, M. Deselnicu, H. Fan, C. Mukarakate, I. Ionescu, S.A. Reid, *Phys. Chem. Chem. Phys.* 8 (2006) 707–713.
- [42] H.H. Nielsen, *Rev. Mod. Phys.* 23 (1951) 90–136.